

NICA-MPD: azimuthal and femtoscopic particle correlations

V.A. Okorokov ^a

National Research Nuclear University “MEPhI” (Moscow Engineering Physics Institute),
Kashirskoe Shosse 31, 115409 Moscow, Russian Federation

Received: date / Revised version: date

Abstract. Discussion is focused on the study of the fundamental symmetries (\mathcal{P}/\mathcal{CP}) of QCD and geometry of the particle source. The combination of correlators corresponded to the absolute asymmetry of distribution of electrically charge particles with respect to the reaction plane in heavy ion collisions is studied. Significant decrease of the absolute asymmetry is observed in intermediate energy range which can be considered as indication on possible transition to predominance of hadronic states over quark-gluon degrees of freedom in the mixed phase created in heavy ion collisions at intermediate energies. For investigation of the energy evolution of geometric properties of particle source the using of femtoscopic radii scaled on the averaged radius of colliding ions is suggested. This approach allows the expansion of the set of interaction types, in particular, on collisions of non-symmetrical ion beams which can be studied within the framework of common treatment. There is no sharp changing of femtoscopic parameter values with increasing of initial energy. The suggestions are made for future advancement of these studies on NICA-MPD.

PACS. 25.75.-q Relativistic heavy-ion collisions, 25.75.Gz Particle correlations and fluctuations

1 Introduction

There is a fundamental interrelation between geometry and fundamental properties of QCD Lagrangian. The vacuum of QCD is a very complicated matter with rich structure, which can corresponds to the fractal-like geometry [1]. Of particular interest of the studies of nucleus-nucleus collisions is a possibility to create a new state of strongly interacting matter where some of the fundamental symmetries may be violated. The non-trivial topology of QCD vacuum opens the possibility for existence of metastable domains which possess of various properties with respect to the discrete \mathcal{P}/\mathcal{CP} symmetries. According to predictions of the theory at finite temperature [2] decays of such domains or classical transitions (sphalerons) between them in deconfinement phase of color charges with restored chiral symmetry can result in local topologically induced violation of \mathcal{P}/\mathcal{CP} invariance in strong interactions – $ITIP$ effect. In the presence of background Abelian electromagnetic field the $ITIP$ effect can leads to the separation of secondary charged particles toward the magnetic field [3, 4]. This phenomenon called also chiral magnetic effect (CME) is the experimental manifestation of the local topologically induced \mathcal{P}/\mathcal{CP} parity violation in the strong interactions. On the other hand, at present femtoscopic measurements in particular that based on Bose–Einstein correlations are unique experimental method for the determination of sizes and lifetimes of sources, i.e. 4D ge-

ometry, in high energy and nuclear physics. The study of nucleus-nucleus ($A + A$) collisions in wide energy domain by correlation femtoscopy seems important for better understanding both the equation of state (EOS) of strongly interacting matter and general dynamic features of soft processes. Therefore, the future experimental studies of non-trivial structure of the QCD vacuum and geometry of particle source in the NICA-MPD energy domain allow the important progress with regard of fundamental symmetries and non-perturbative properties of the strong interactions.

2 Fundamental symmetries of QCD at finite temperature

With taking into account possible local strong \mathcal{P}/\mathcal{CP} violation the invariant distribution of final state particles with certain sign of electric charge α ($\alpha = +, -$) can be written as following

$$E \frac{d^3 N_\alpha}{d\mathbf{p}} = \frac{1}{2\pi} \frac{d^2 N_\alpha}{p_\perp dp_\perp dy} \left[1 + 2 \sum_{n=1}^{\infty} \sum_{m=1}^2 k_{n,\alpha}^m F^m(n\Delta\phi) \right].$$

Here $\Delta\phi \equiv \phi - \Psi_{RP}$, ϕ is an azimuthal angle of particle under study, Ψ_{RP} – azimuthal angle of reaction plane, $F^{1,2}(x) \equiv \cos(x), \sin(x)$, $k_{n,\alpha}^1 \equiv v_{n,\alpha}$ – collective flow of n -th order, the parameters $k_{n,\alpha}^2 \equiv a_{n,\alpha}$ describe the effect of \mathcal{P}/\mathcal{CP} violation. It should be emphasized that the

^a e-mail: VAOkorokov@mephi.ru; Okorokov@bnl.gov

CME is the collective effect and its investigation is possible via correlation analysis only because the $\langle a_{n,\alpha} \rangle = 0$ if the one-particle distributions are averaged over event sample. According to the theory, the correlator contained the contribution of possible $\mathcal{P}/\mathcal{C}\mathcal{P}$ violation effect only is given by equation $\langle \mathbf{K}_{n,\alpha\beta}^T \rangle = \langle a_{n,\alpha} a_{n,\beta} \rangle$, where α, β – the electric charge signs of secondary particles. Only the first harmonic coefficient is analyzed so far because as expected the $a_{1,\alpha}$ accounts for most of the effect under study. Thus the following notation $\langle \mathbf{K}_{1,\alpha\beta}^T \rangle \equiv \langle \mathbf{K}_{\alpha\beta}^T \rangle$ is used below. The structure of the $\langle \mathbf{K}_{\alpha\beta}^T \rangle$ is described in detail elsewhere [3, 5]. Experimental correlator proposed in [6] is defined as following $\langle \mathbf{K}_{\alpha\beta}^E \rangle = \langle \cos(\phi_\alpha + \phi_\beta - 2\Psi_{RP}) \rangle$. This observable is sensitive to the effect of possible local strong $\mathcal{P}/\mathcal{C}\mathcal{P}$ violation and measures the charge separation with respect to the reaction plane. Both theoretical and experimental correlators are averaged over pairs of particles under study in event and over all events in sample. It should be mentioned that correlators defined above are \mathcal{P} -even quantities therefore the $\langle \mathbf{K}_{\alpha\beta}^E \rangle$ may contains contributions from background effects unrelated to possible local strong $\mathcal{P}/\mathcal{C}\mathcal{P}$ violation. Theoretical and experimental correlators are related by following equation

$$\langle \mathbf{K}_{\alpha\beta}^E \rangle = B - \langle \mathbf{K}_{\alpha\beta}^T \rangle, \quad (1)$$

where B is the total background contribution discussed in [5]. The absolute asymmetry with respect to the reaction plane for azimuthal distribution of electric charges in final state is define as following [5]

$$A_a = -[\langle \mathbf{K}_{\pm\pm}^E \rangle - \langle \mathbf{K}_{\mp\mp}^E \rangle]. \quad (2)$$

In the framework of CME model [3] for ideal case of chiral limit and an extremely large magnetic field the following relations have been derived [5]

$$\langle Q^2 \rangle \propto \Gamma_{CS}, \quad A_a \propto \Gamma_{CS}. \quad (3)$$

Here $\langle Q^2 \rangle$ is the average square of charge difference (in units of e) between opposite sides of the reaction plane, Γ_{CS} is the classical transition rate, i.e. the Chern–Simons diffusion rate. It should be noted that separation of possible CME signal from background effects is an important and difficult task for $\langle \mathbf{K}_{\alpha\beta}^E \rangle$ and consequently for A_a quantity. Based on the available experimental results and its interpretation for wide initial energy range one can assume at qualitative level only that the sizable contribution in A_a will be due to correlations driven by local $\mathcal{P}/\mathcal{C}\mathcal{P}$ violation in strong interactions [5].

Fig. 1 shows the energy dependence of A_a for semi-central events in various bins of centrality for heavy ion beams. The equation for Chern–Simons diffusion rate for case of finite B had been derived in [7]. Background magnetic field typically created in relativistic heavy ion collisions is characterized by the strength $B \sim T^2$ [3, 8, 9]. The regime of finite external magnetic field is investigated in the paper and it is observed that the curves for $B = 0$ and for case $B = T^2$ coincide completely for all centrality bins under study, i.e. for full centrality domain 20-60%

shown in Fig. 1. But relations in (3) have been obtained for extremely strong magnetic field. Thus energy dependence for Chern–Simons diffusion rate are computed for external Abelian magnetic field with various strengths as following [7]

$$\Gamma_{CS}^{B \neq 0} = \Gamma_{CS}^{B=0} [1 + \zeta^2 / (6\pi^4)], \quad \zeta \equiv B/T^2.$$

It would be noted that at fixed ζ functional dependence of Γ_{CS} on T is the same both for $B = 0$ and for general case of presence of finite external Abelian magnetic field. The function suggested in [10] for description of energy dependence of chemical freeze-out temperature agrees with available experimental data quite reasonable for energies up to $\sqrt{s_{NN}} = 200$ GeV [11] and for all centralities [12] under study. Therefore the analytic dependence $T(\sqrt{s_{NN}})$ from [10] is used for estimations of Γ_{CS} in energy domain under study. The smooth curves in Fig. 1 are the energy dependencies of Chern–Simons diffusion rate in the strong coupling regime at $B = 0$ (solid), $B = 5T^2$ (dashed) and $B = 10T^2$ (dotted). The norm for solid curves is the STAR point for Au+Au at $\sqrt{s_{NN}} = 200$ GeV. The shaded bands for Chern–Simons diffusion rate at $B = 0$ are defined by uncertainties of T value at fixed initial energy due to errors of parameters in analytical function described of $T(\sqrt{s_{NN}})$ experimental dependence [10]. As seen, phenomenological curves $\Gamma_{CS}(\sqrt{s_{NN}})$ are in area caused by spread of T values at fixed $\sqrt{s_{NN}}$ for following wide range of changing of strength of external Abelian magnetic field $B \leq 5T^2$ at any initial energies under study, moreover at $\sqrt{s_{NN}} \lesssim 12$ GeV – for all range of changing of B under considered in Fig. 1. Functional behavior of $\Gamma_{CS}(\sqrt{s_{NN}})$ does not depend on B in high energy domain at changing of B on order of magnitude at least.

One sees the some decreasing of A_a for LHC energy as compared to initial energy domain $\sqrt{s_{NN}} \sim 100$ GeV, the absolute value of decreasing growths for more peripheral events. The parameter A_a goes down significantly with $\sqrt{s_{NN}}$ decreasing for intermediate initial energy domain 7.7 – 20 GeV in semi-central heavy ion collisions (Fig. 1). For each centrality bin under study the estimations for $A_a(\sqrt{s_{NN}})$ correspond to the energy dependence of Γ_{CS} at $B = 0$ on qualitative level with some enhancement of experimental points over phenomenological curves in range $\sqrt{s_{NN}} \sim 20 - 40$ GeV for events with 20-30% (Fig. 1a) and 30-40% (Fig. 1b) centrality. Perhaps, for better description of $A_a(\sqrt{s_{NN}})$ at $\sqrt{s_{NN}} \sim 20 - 40$ GeV the influence of external B on Γ_{CS} should be taken into account. This suggestion agrees with dependence of B on initial energy [8] which demonstrates that B in intermediate energy range $\sqrt{s_{NN}} \sim 20 - 40$ GeV reaches very large values with respect to the strength of B at $\sqrt{s_{NN}} \sim 100$ GeV. The qualitative agreement is observed between values of A_a parameter calculated for Au+Au collisions and phenomenological curves for any strength values B under study. This feature can be considered as some evidence of validity of relations in (3) derived at ultimate strong external Abelian magnetic field for heavy ion collisions. Decreasing of $\Gamma_{CS}(\sqrt{s_{NN}})$ observed at $\sqrt{s_{NN}} < 20$ GeV should leads to attenuation of CME and its manifestation

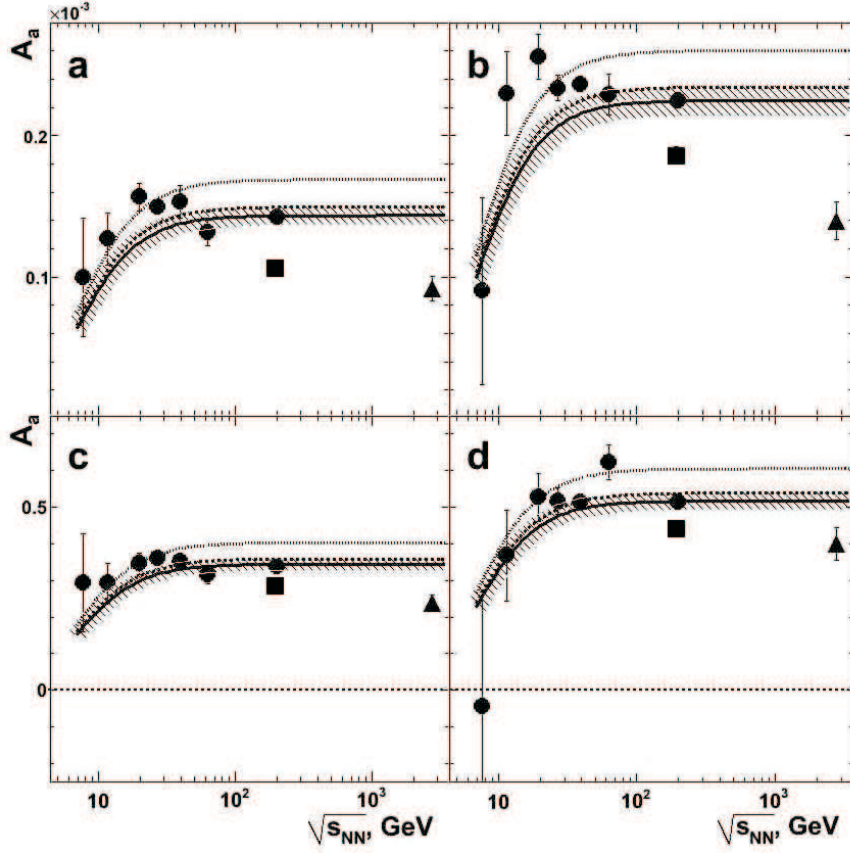


Fig. 1. Energy dependence of A_a for heavy ion collisions in various centrality bins: a – 20-30%, b – 30-40%, c – 40-50% and d – 50-60% [5]. Experimental points are shown as following: ● – Au+Au, ▲ – Pb+Pb and ■ – U+U. Smooth curves correspond to the energy dependence of Chern–Simons diffusion rate in the strong coupling regime for external magnetic field with strength $B = 0$ (solid), $B = 5T^2$ (dashed) and $B = 10T^2$ (dotted). The shaded areas for Γ_{CS} at $B = 0$ are defined by uncertainties of T value at fixed initial energy due to errors of parameters in analytic function described of $T(\sqrt{s_{NN}})$ experimental dependence.

on experiment at intermediate energies. Taking into account conditions which are essential for CME one can suppose the following hypothesis. The changing of behavior of dependence $A_a(\sqrt{s_{NN}})$ observed at transition from high energy domain down to intermediate energy range may be driven by predominance of hadronic colorless states over quark-gluon deconfinement phase at $\sqrt{s_{NN}} < 19.6$ GeV and, as consequence, by decreasing of CME. Thus behavior of experimental quantity A_a vs collision energy agrees with qualitative expectation for transition to the predominance of hadronic phase in domain $\sqrt{s_{NN}} < 19.6$ GeV and with decreasing of Chern–Simons diffusion rate at intermediate initial energies.

3 Femtoscopic correlations

The discussion below is focused on specific case of femtoscopic, namely, on correlations in pairs of identical charged pions with small relative momenta – HBT-interferometry – in $A + A$ collisions. The set of main femtoscopic

observables $\mathcal{G} \equiv \{\mathcal{G}_1^i\}_{i=1}^4 = \{\lambda, R_s, R_o, R_l\}$ is only under consideration here. The \mathcal{G} characterizes the correlation strength and source’s 4-dimensional geometry at freeze-out stage completely, some important additional observables which can be calculated with help of HBT radii are discussed elsewhere [13,14]. The most central collisions are usually used for study the space-time characteristics of final-state matter, in particular, for discussion of global energy dependence of femtoscopic observables. Therefore scaled parameters \mathcal{G}^i , $i = 2 - 4$ are calculated as following [13]:

$$R_i^n = R_i/R_A, \quad i = s, o, l. \quad (4)$$

Here $R_A = R_0 A^{1/3}$ is radius of spherically-symmetric nucleus, $R_0 = (1.25 \pm 0.05)$ fm [15]. The change $R_A \rightarrow \langle R_A \rangle = 0.5(R_{A_1} + R_{A_2})$ is made in the relation (4) in the case of non-symmetric nuclear collisions [13]. In general case the scale factor in (4) should takes into account the centrality of nucleus-nucleus collisions. The normalization procedure suggested in [13] allows the general consideration of all available data for nucleus-nucleus collisions

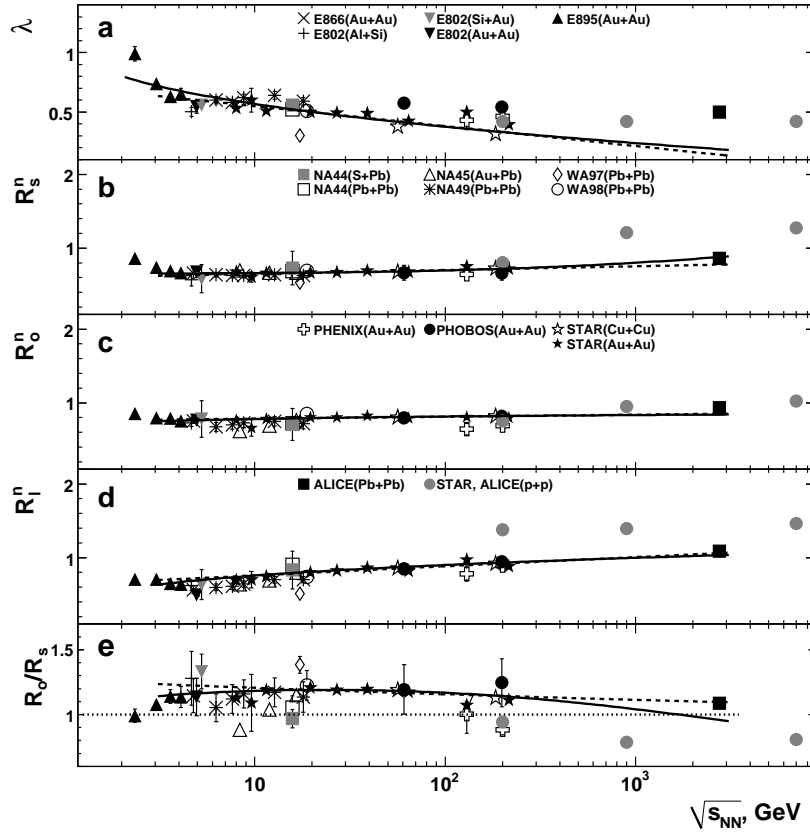


Fig. 2. Energy dependence of λ parameter (a), scaled HBT-radii (b – d) and ratio R_o/R_s (e) in various collisions. Experimental data are from [14]. Statistical errors are shown (for NA44 – total uncertainties). The solid lines (a – d) correspond to the fits by function (5) and dashed lines – to the fits by specific case of (5) at fixed $a_3 = 1.0$. Smooth solid and dashed curves at (e) correspond to the ratio R_o/R_s calculated from the fit results for R_s^n and R_o^n in $A + A$, dotted line is the level $R_o/R_s = 1$.

together with the proton-proton (pp) results at high energies with replacing $R_A \rightarrow R_p$ in (4). Detail study for (quasi)symmetric heavy ion collisions [13] demonstrates that the fit function ($\varepsilon \equiv s_{NN}/s_0$, $s_0 = 1 \text{ GeV}^2$)

$$f(\sqrt{s_{NN}}) = a_1 [1 + a_2 (\ln \varepsilon)^{a_3}] \quad (5)$$

agrees reasonably with experimental $\mathcal{G}^i(\sqrt{s_{NN}})$, $i = 1 - 4$ at any collision energy for λ and at $\sqrt{s_{NN}} \geq 5 \text{ GeV}$ for HBT radii. Fig. 2 shows the energy dependence of λ (a), scaled HBT-radii (b – d) and R_o/R_s ratio (e) for both the symmetric and non-symmetric collisions of various nuclei. Fits of experimental dependencies for $A + A$ interactions are made by (5) in the same energy domains as well as for (quasi)symmetric heavy ion collisions. Fit curves are shown in Fig. 2 by solid lines for (5) and by dashed lines for specific case of fit function at $a_3 = 1.0$ with taking into account statistical errors. The fit by (5) underestimates the λ value at the LHC energy $\sqrt{s_{NN}} = 2.76 \text{ TeV}$ significantly. The λ values for asymmetric nucleus-nucleus collisions at intermediate energies $\sqrt{s_{NN}} \lesssim 20 \text{ GeV}$ agree well with values of λ in symmetric heavy ion collisions at close

energies. On the other hand the development of some approach is required in order to account for type of colliding beams in the case of λ parameter and improve quality of approximation. Smooth curves for normalized HBT radii and ratio R_o/R_s are in reasonable agreement with experimental dependencies in fitted domain of collision energies $\sqrt{s_{NN}} \geq 5 \text{ GeV}$ (Figs. 2b – e). The scaled HBT-radii in pp are larger significantly than those in $A + A$ collisions at close energies. Because feature of Regge theory [16] the following relation is suggested to take into account the expanding of proton with energy: $R_p = r_0(1 + k\sqrt{\alpha'_p \ln \varepsilon})$, where $r_0 = (0.877 \pm 0.005) \text{ fm}$ is the proton's charge radius [17], parameter $\alpha'_p \propto \ln \varepsilon$ because of diffraction cone shrinkage speeds up with collision energy in elastic pp scattering [18]. The k is defined from the boundary condition $R_p \rightarrow 1/m_\pi$ at $\varepsilon \rightarrow \infty$ with choice of appropriate asymptotic energy $\sqrt{s_{NN}^a}$. The detail study demonstrates that the increasing of $\sqrt{s_{NN}^a}$ from 6 PeV [19] to 10^3 PeV influences weakly on R_i^n , $i = s, o, l$ in pp collisions and calculations are made for the first case. The normalized transverse radii agree in both the pp and the $A + A$ collisions

(Figs. 2b, c) at $\sqrt{s_{NN}} = 200$ GeV with excess of R_s^n in pp with respect to the $A + A$ in TeV-region. The R_l^n in pp is larger than that for $A + A$ in domain $\sqrt{s_{NN}} \geq 200$ GeV. It should be stressed that the additional study is important, at least, for choice of $R_p(\varepsilon)$.

4 Future investigations

It should be noted that the requirements for main tracker of MPD – time-projection chamber – give the possibility for measurements of various correlations, in particular discussed above, with high quality and statistic.

The study at NICA-MPD with heavy ion beams allows the precise measurement of the $A_a(\sqrt{s_{NN}})$ dependence in energy region of sharp decrease of absolute asymmetry. These future investigations will be useful for test of the hypothesis about attenuation of the CME due to transition to the predominance of hadronic phase in domain $\sqrt{s_{NN}} < 19.6$ GeV. Furthermore in this paper it is suggested that at finite temperature (T) the transition rate between vacuum states with different N_{CS} is dominated by transition rate due to sphalerons only, without consideration of exponentially suppressed transitions due to instantons. But it would be mentioned that some additional study and justification may be required for this approach, especially in temperature range $T_c < T < 3T_c$ [20], where T_c – temperature of phase transition to the deconfinement state of color charges. The such investigations can be proposed for NICA-MPD physics program.

New experimental data are important for verification of the suggestion of separate dependencies $\lambda(\sqrt{s_{NN}})$ for moderate and heavy ion collisions. The energy dependence is almost flat for the scaled difference $\delta^n \equiv (R_o^2 - R_s^2)R_A^{-2}$ in $A + A$ collisions within large error bars [13,14]. The indication on possible curve knee at $\sqrt{s_{NN}} \sim 10 - 20$ GeV obtained in the STAR high-statistics data agree with other results in the framework of the phase-I of the BES program at RHIC. But additional precise measurements at NICA-MPD with various beams and $\sqrt{s_{NN}}$ may be crucially important in order to confirm this feature in energy dependence of important parameter δ^n . Furthermore there is wide set of femtoscopic measurements available at NICA-MPD with both the identical heavier particles and the non-identical particle pairs. The $\Lambda\Lambda$ correlations can be used for search for exotic states in QCD, for instance, H dibaryons [21]. The non-identical particle correlations with kaons allow us to obtain information about space-time asymmetry of particle emission, final state interaction, some exotic objects like kaonic atoms.

5 Summary

The absolute asymmetry is introduced in order to investigate the evolution of CME in heavy ion collisions with initial energy. Dependence on $\sqrt{s_{NN}}$ has been obtained for A_a based on the experimental correlators. The energy dependence of absolute asymmetry for semi-central events

in heavy ion collisions shows sharp decreasing at $\sqrt{s_{NN}} < 19.6$ GeV, almost constant behavior up to $\sqrt{s_{NN}} \simeq 200$ GeV with some decreasing at further energy increasing. Dependence $A_a(\sqrt{s_{NN}})$ qualitatively corresponds to the energy dependence of Chern–Simons diffusion rate. The $A_a(\sqrt{s_{NN}})$ indicates possibly on the onset of predominance of hadronic states versus phase of color degrees of freedom in deconfinement state in the matter created in heavy ion collisions with initial energies from domain $\sqrt{s_{NN}} \lesssim 11.5 - 19.6$ GeV. Energy dependence is investigated for the main femtoscopic parameters deduced in the framework of Gauss approach. There is no dramatic change of femtoscopic parameter values in $A + A$ with increasing of $\sqrt{s_{NN}}$ in domain of collision energies $\sqrt{s_{NN}} \geq 5$ GeV. The normalized some HBT radii in pp are larger significantly than those in $A + A$ collisions especially in TeV-region. The fit curves demonstrate qualitative agreement with experimental $A + A$ data for λ at all available collision energies and for normalized HBT radii in energy domain $\sqrt{s_{NN}} \geq 5$ GeV.

The investigations of azimuthal and femtoscopic correlations at intermediate energies with high statistics at NICA-MPD can provide new important information for better understanding of structure of the QCD vacuum as well as relation between geometry and dynamic features of creation of the secondary particle source. The correlation measurements can be one of the focuses and significant part of the NICA-MPD physics program.

References

1. V.A. Okorokov, E.V. Sandrakova, Univ. J. Phys. Appl. **1**, 196 (2013).
2. T.D. Lee, Phys. Rev. D **8**, 1226 (1973); T.D. Lee, G.G. Wick, Phys. Rev. D **9**, 2291 (1974).
3. D.E. Kharzeev *et al.*, Nucl. Phys. A **803**, 227 (2008).
4. K. Fukushima *et al.*, Phys. Rev. D **78**, 074033 (2008).
5. V.A. Okorokov, Int. J. Mod. Phys. E **22**, 1350041 (2013).
6. S.A. Voloshin, Phys. Rev. C **70**, 057901 (2004).
7. G. Basar, D.E. Kharzeev, arXiv: 1202.2161 [hep-ph].
8. V.A. Okorokov, arXiv: 0908.2522 [nucl-th]; V.A. Okorokov, Phys. At. Nucl. Eng. **4**, 805 (2013).
9. V.V. Skokov *et al.*, Int. J. Mod. Phys. A **24**, 5925 (2009); V. Voronyuk *et al.*, Phys. Rev. C **83**, 054911 (2011).
10. J. Cleymans *et al.*, Phys. Rev. C **73**, 034905 (2006).
11. M.M. Aggarwal *et al.*, Phys. Rev. C **83**, 024901 (2011).
12. L. Kumar, Nucl. Phys. A **904-905**, 256c (2013).
13. V.A. Okorokov, arXiv: 1312.4269 [nucl-ex]. 2013; V.A. Okorokov, Adv. High Energy Phys. **2015**, 790646 (2015).
14. V.A. Okorokov, arXiv: 1504.08336 [nucl-ex].
15. L. Valentin, *Subatomic physics: nuclei and particles V. I* (Ermann, Paris, 1982); K.N. Mukhin, *Experimental nuclear physics V. I* (Energoatomizdat, Moscow, 1993).
16. P. Collins, *An introduction to Regge theory and high energy physics* (Cambridge Univ. Press, Cambridge, 1977).
17. K.A. Olive *et al.*, Chin. Phys. C **38**, 090001 (2014).
18. V.A. Okorokov, Adv. High Energy Phys. **2015**, 914170 (2015).
19. C. Bourrely *et al.*, arXiv: 1202.3611 [hep-ph]. 2012.
20. E.-M. Ilgenfritz, E.V. Shuryak, Phys. Lett. B **325**, 263 (1994).
21. C. Greiner, B. Müller, Phys. Lett. B **219**, 199 (1989).